Comparative Study of Low-Pass Filter and Phase-Locked Loop Type Speed Filters for Sensorless Control of AC Drives

Dong Wang, *Member, IEEE*, Kaiyuan Lu, *Member, IEEE*, Peter Omand Rasmussen, *Member, IEEE*, and Zhenyu Yang, *Member, IEEE*

***Abstract*—High quality speed information is one of the key issues in machine sensorless drives, which often requires proper filtering of the estimated speed. This paper comparatively studies typical low-pass filters (LPF) and phase-locked loop (PLL) type filters with respect to ramp speed reference tracking and steady-state performances, as well as the achievement of adaptive cutoff frequency control. An improved LPF-based filter structure with no ramping and steady-state errors caused by filter parameter quantization effects is proposed, which is suitable for applying LPF for sensorless drives of AC machines, especially when fixed-point digital signal processor is selected e.g. in mass production. Furthermore, the potential of adopting PLL for speed filtering is explored. It is demonstrated that PLL type filters can well maintain the advantages offered by the improved LPF. Moreover, it is found that the PLL type filters exhibit almost linear relationship between the cutoff frequency of the PLL filter and its proportional-integral (PI) gains, which can ease the realization of speed filters with adaptive cutoff frequency for improving the speed transient performance. The proposed filters are verified experimentally. The PLL type filter with adaptive cutoff frequency can provide satisfactory performances under various operating conditions and is therefore recommended.**

***Index Terms*—Adaptive cutoff frequency, low-pass filter, machine sensorless drive, phase-locked loop, speed filter, static error**

I. Introduction

SENSORLESS control of AC drives has been extensively studied in the last three decades. Many research efforts have been dedicated to propose reliable and accurate methods for rotor position estimation [1-3], which plays a crucial role in realizing field oriented control (FOC) of various types of AC drives. Rotor position estimation may be accomplished in every switching period for algorithms based on fundamental- or continuous high frequency signal excitations [4-12], or in only few switching periods for discontinuous high frequency signal injection based algorithms [13-15]. With the position estimation algorithm involved, it was still possible to realize high bandwidth control of the current loop [13].

Besides the position estimation, fast and accurate speed estimation is another key issue required for high performance sensorless AC drives. Accurate speed signal with low disturbances can provide smooth feedback to the speed regulator and consequently reliable current commands for the inner current control loops. The whole drive system may then work without undesired current and torque ripples. The drive may track the speed reference more accurately with minimized steady-state speed ripple.

At the early development stage of sensorless drives, the speed information was simply obtained from the derivative of the estimated position [4], or from the machine mechanical model [5]. Such obtained speed signal may have a high noise ratio, resulting in high current disturbances and may not be appropriate for speed feedback in a sensorless drive system [6]. A better solution was proposed to use a phase-locked loop (PLL) to handle the estimated position or position error to generate a better position signal and in the meantime, relatively better speed signal may be achieved [7-14]. Such PLL has been studied in details in [7], [8], and has become a very popular solution [9-14]. However, though the speed obtained from the PLL has better noise suppression ability than the derivative operation, the speed noise can still be high, e.g. when large proportional-integral (PI) gains are used in the PLL handling fast mechanical dynamics such as speed reversal or step load change. To overcome this problem, in [10], additional acceleration component obtained from the machine mechanical model was used together with the PLL. Small PI gains may then be used to suppress the noise without sacrificing the performance of the drive too much during transient processes. However, the machine mathematical models and parameters are required in this method to predict the performance during transients and several gain units in the observer need to be carefully tuned before satisfactory results can be achieved. In this method, mechanical parameters of the drive are also needed. Their acquisition often needs complicated control of the drive to follow e.g. sinusoidal speed reference [16]. This makes the methods requiring mechanical parameters not easy to be implemented. It is therefore needed to investigate if there is any simple speed filter that may give improved speed filtering performance, especially for applications that do not require fast shaft dynamics, such as applications with fan, pump, and compressor types of loads.

A first order infinite impulse response (IIR) low-pass filter

This work was supported in part by Lodam A/S and in part by the PSO-ELFORSK Program.

The authors are with the Department of Energy Technology, Aalborg University, Aalborg, DK-9220, Denmark (e-mail: dwa@et.aau.dk; klu@et.aau.dk; por@et.aau.dk; yang@et.aau.dk).

(LPF) was employed to filter the estimated speed for permanent magnet (PM) machines [4], [6]. However, significant delay was observed during speed ramp even with compensation technique, which requires machine parameters to help with the speed estimation. Moreover, there are several practical problems need to be considered when realizing a digital LPF, such as the quantization errors [17], especially for the widely used fixed-point digital signal processor (DSP) in mass production, which is known with the round-off error problem [18]. It should be noted that the coefficients of the digital filter requires a high word-length; otherwise, accumulation error will appear and may cause system to become unstable [17]. Therefore, a normal LPF is not an ideal choice for speed filtering, especially when fixed-point DSP is adopted. Therefore, effort is still needed to find a simple but effective speed filter and its implementation should be model/parameter independent.

In this paper, normal LPF is first discussed and its ramp speed tracking error and steady-state error due to filter parameter quantization are illustrated. An improved LPF-based speed filter structure is then proposed. Compared to the normal LPF, the proposed solution can track a ramp speed reference more accurately and it generates no steady-state error caused by parameter quantization effects. Another type of filter that is based on the PLL structure is analyzed afterwards. The study has shown that it can overcome the above mentioned drawbacks associated to normal LPFs, i.e. possible accumulation error in steady-state and ramp response error (time delay). In additional, PLL type filters exhibit almost linear relationship between the cutoff frequency and the PI gains in the PLL. This is a very promising feature that can ease the realization of speed filters with adaptive cutoff frequency that can improve the speed transient performance. Experimental verifications are given to support the analysis carried out in this paper. Good performance at steady-state and satisfactory performance during speed transients are obtained.

II. Control Scheme Overview

A synchronous reluctance machine (SynRM) drive system is chosen to carry out all the investigations in this paper, due to the availability in the lab. The complete system topology of the sensorless control, including the open-loop *I-f* startup procedure and the closed-loop field-oriented control (FOC), is illustrated in Fig. 1. The three switches are connected to terminal 1 during the open-loop startup procedure and switched to terminal 2 during normal FOC operation. The open-loop *I-f* startup strategy, which is used to accelerate the SynRM from zero speed to a preset switching over speed, e.g. 20% of the machine rated speed, was initially introduced for permanent magnet synchronous machine (PMSM) and detailed stability analysis and design guidelines were given in [19]. After the SynRM has reached the preset switching over speed, the controller is then switched to the closed-loop FOC operation.

A PLL is often used in the sensorless controller in the position and speed observer block (Fig. 1) for e.g. recovering the position information from the estimated position error. It is worth to notice that PLL has low-pass filter features. For sensorless algorithms that estimate the position (not position error) directly, a PLL is still employed to filter the noise of the estimation position and in the meantime, the speed may also be estimated [7-14].

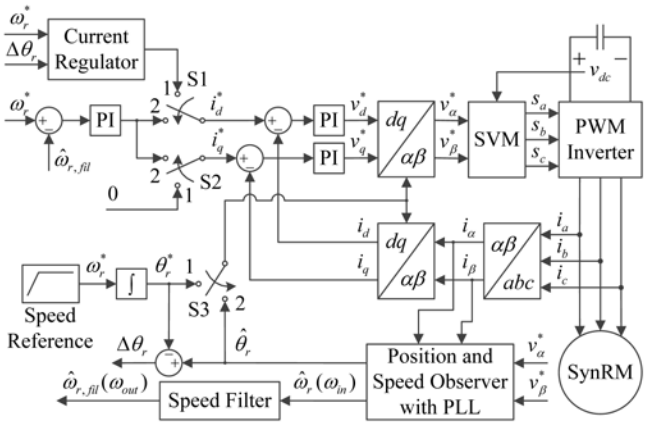

Fig. 1. Position sensorless control scheme with startup procedure for SynRM.

The PLL used in the position and speed observer is mainly used for position estimation purpose. When large PI gains are chosen to handle fast mechanical dynamics, the speed obtained from this PLL is often noisy, which is shown experimentally later in this paper. Thus, extra speed filters may be needed to obtain a better speed signal. Fig. 2 illustrates all the filter structures that are investigated in this paper, where ω_{in} and ω_{out} correspond to $\hat{\omega}_r$ and $\hat{\omega}_{r,fil}$ respectively shown in Fig. 1.

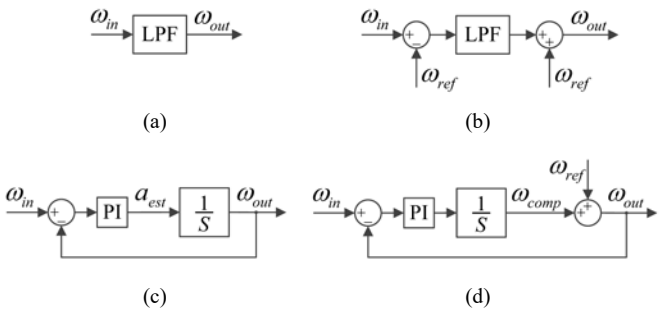

Fig. 2. Filter structures. (a) Normal LPF structure. (b) Improved LPF-based structure. (c) Normal PLL structure. (d) Modified PLL-based structure.

III. LPF Based Filter Structures

A LPF is a typical option for extra speed filtering and the possible filter structures are analyzed in this section.

A. Normal LPF Characteristics

The LPF used in Fig. 2(a) could be a first order IIR LPF or higher order IIR LPFs. A normal first order IIR LPF can be represented as

$$H_{LPF1}(s)=\frac{\omega_{out}(s)}{\omega_{in}(s)}=\frac{1}{Ts+1}, \quad (1)$$

where T is the time constant, ω_{in} and ω_{out} are input and output speed of the LPF respectively. The cutoff frequency of the LPF can be calculated as

$$f_c=1/(2\pi T). \quad (2)$$

The transfer function of a normal second order IIR LPF which offers better filtering effects can be represented as

$$H_{LPF2}(s)=\frac{\omega_{out}(s)}{\omega_{in}(s)}=\frac{1}{T^2s^2+2\zeta Ts+1}, \tag{3}$$

where ζ is the damping factor, which is typically 0.707 for Butterworth filter. The cutoff frequency can be calculated by (2) as well.

It has been verified experimentally in [6] that the normal LPFs can cause large time delay during speed ramps, especially when the cutoff frequency is low. The constant time delay is equivalent to a constant speed error ($\varepsilon=\omega_{in}-\omega_{out}$), which can be calculated as

$$\varepsilon(s)=\left(1-H_{LPF}(s)\right)\cdot\omega_{in}(s), \tag{4}$$

For fixed or step inputs, this error converges to

$$\lim_{t\to\infty}\varepsilon=\lim_{s\to0}s\varepsilon(s)=\lim_{s\to0}s\left(1-H_{LPF}(s)\right)\cdot\frac{\omega_{in}}{s}=0, \tag{5}$$

This is valid for both the first and second order LPFs.

However, for ramp input $\omega_{in}=a_{in}\cdot t$, where a_{in} is the slope/acceleration ratio of ω_{in}, the error of the first order LPF during the ramp procedures converges to

$$\lim_{t\to\infty}\varepsilon=\lim_{s\to0}\left(s\left(1-\frac{1}{Ts+1}\right)\cdot\frac{a_{in}}{s^2}\right)=\lim_{s\to0}\frac{Ta_{in}}{Ts+1}=Ta_{in}, \tag{6}$$

which has been examined experimentally in [6]. Regarding the second order LPF, the ramp error converges to

$$\lim_{t\to\infty}\varepsilon=\lim_{s\to0}\left(s\frac{T^2s^2+2\zeta Ts}{T^2s^2+2\zeta Ts+1}\cdot\frac{a_{in}}{s^2}\right)=2\zeta Ta_{in}. \tag{7}$$

This suggests that for LPF, there will always be errors when tracking ramp speed signal.

Another problem for LPF is that accumulation error may exist at steady-state conditions due to the quantization errors of the coefficients of the digital filter [17]. For applications with fixed-point DSP, the round-off error during the calculation will worsen the situation and result in even higher steady-state error. This important phenomenon is demonstrated in Fig. 3(a) and (b), where a second order IIR LPF with a cutoff frequency of f_c =5 Hz is investigated as an example in order to observe clear errors. Two digital filters are obtained from the original analog LPF: one with high-precision coefficients that have sixteen significant figures (named as "dLPF2_h"); the other one with low-precision coefficients that have seven significant figures (named as "dLPF2_l"). These filters are applied to the SynRM drive system with a ramp change of the reference speed. It can be seen from Fig. 3(a) that there is no errors for digital filter "dLPF2_h" in steady-state; while steady-state error exists for digital filter "dLPF2_l" as shown in Fig. 3(b), which reaches 23 rpm after ramping up to 1500 rpm. Besides, it can be seen that there is a constant speed error (time delay) during the ramp procedure for both digital filters "dLPF2_h" and "dLPF2_l". Theoretically, according to (7), for this example with $a_{in}\approx a_{ref}$= 500 rpm/s and ζ= 0.707, the constant error during the ramp procedure of "dLPF2_h" is $\varepsilon=2\zeta Ta_{in}\approx$22.5 rpm, which may be observed from Fig. 3(a). It should be pointed out that the speed

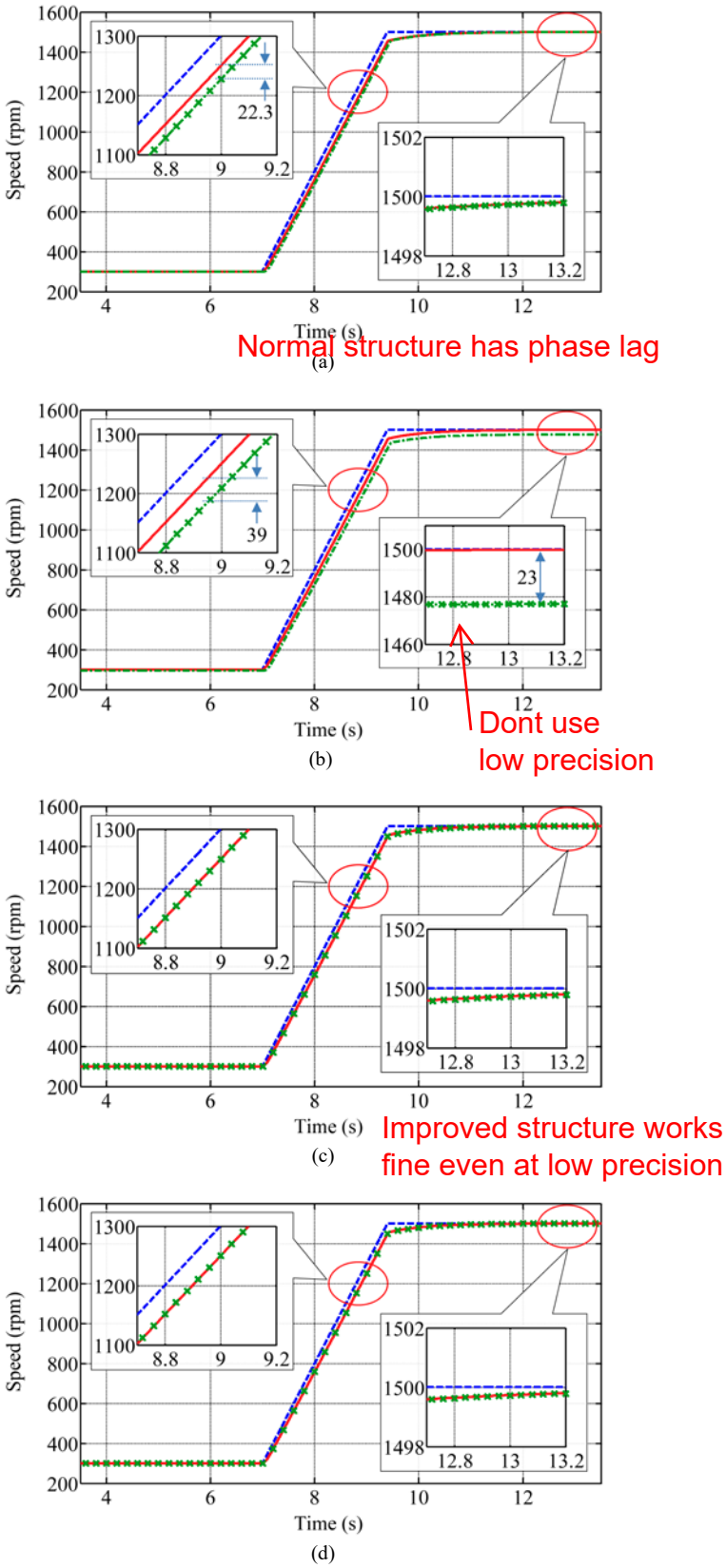

Fig. 3. Simulated performance of second order LPFs with f_c=5 Hz: reference speed (blue dashed line); input speed (solid red line); output speed after digital LPF (green dash-dot line with "x" marker). (a) High-precision coefficients digital filter "dLPF2_h" with normal structure. (b) Low-precision coefficients digital filter "dLPF2_l" with normal structure. (c) "dLPF2_h" with improved structure. (d) "dLPF2_l" with improved structure.

filter itself will cause system delay. Therefore, it is most suitable for applications that do not require fast shaft dynamics. A ramp speed reference that can be followed closely by the machine is surely acceptable in these applications.

B. Improved LPF-Based Filter Structure

The error in tracking a ramp speed input and the steady-state error due to filter parameter quantization effects mentioned above may be overcome by using the proposed speed filter structure shown in Fig. 2(b).

In Fig. 2(b), the input speed to be filtered is first subtracted by the reference speed and the same reference speed is added to the output of the LPF. The error of the improved LPF can be calculated as

$$\varepsilon(s) = \left(1 - H_{LPF}(s)\right) \cdot \left(\omega_{in}(s) - \omega_{ref}(s)\right). \tag{8}$$

There are two advantages by introducing ω_{ref} when filtering with LPFs. First, the second order ramp input ω_{in} can be reduced to a first order input $\omega_{in} - \omega_{ref}$, which eliminates the error during ramping procedure. Secondly, the accumulation error caused by the quantization errors of digitalized filter coefficients will be cancelled out because the accumulation error of inputs ω_{in} and ω_{ref} are the same. From other point of view, a first order constant input ω_{in} is reduced to a zero input $\omega_{in} - \omega_{ref}$, so that ε is zero according to (8). Therefore, introducing of ω_{ref} in the filtering structure with LPFs can eliminate those errors.

The same digital filters "dLPF2_h" and "dLPF2_l" used before are applied in the modified structure (Fig. 2(b)) by introducing ω_{ref}. The same simulation is repeated and the results are shown in Fig. 3(c) and (d). It can be seen that errors are eliminated for both steady state and ramping conditions for those two filters. The two digitalized filters with different parameter accuracies give very similar performances. The improved LPF structure is no-longer sensitive to parameter quantization errors.

IV. PLL Type Based Filter Structures

The main role of the PLL in the existing sensorless drives is for position estimation only. The input to the PLL is the position error and the output of the loop filter (LF) in the PLL is the estimated speed, whose integration gives the estimated position. It has very clear physical meaning, i.e. when the input position error is greater than zero (estimated position is lagging the real position), the LF will increase the output estimated speed, to force the estimated position to approach the real position. Although PLL has demonstrated very good performances in many sensorless drives for position estimation and the speed may be estimated as well, to use its low-pass filtering characteristics for speed filtering purpose has not been well discussed in the existing literatures. When considering filtering the speed, the speed error, instead of position error will be chosen as the input to the PLL.

Fig. 2(c) illustrates the normal structure of a PLL, where a PI regulator is selected to perform as the LF. When it is used for speed filtering, the input should be the original speed to be filtered as illustrated in Fig. 2(c). The physical meaning of the function of the PLL is also clear, i.e. when the estimated speed by the PLL is lower than the original speed to be filtered, the LF will increase its output, which in this case is the estimated speed acceleration ratio a_{est}, whose integration gives the filtered speed signal. Similar to the improved LPF-based filter structure given in Fig. 2(b), the standard PLL structure may be modified to Fig. 2(d), where the reference speed information ω_{ref} is used as an additional input. It should be noticed that the structure shown in Fig. 2(d) is different from the PLL structure involving reference speed used for grid synchronization [20], where the feed-forward reference signal is introduced before the integrator. In the structure given in Fig. 2(d), the reference signal is introduced after the integrator, since when applied for speed filtering, the output of the integrator in Fig. 2(d) is the compensation component ω_{comp}, reflecting the deviation of the estimated speed from the reference speed.

The transfer function of the normal PLL in Fig. 2(c) is

$$H_{PLL}(s) = \frac{\omega_{out}(s)}{\omega_{in}(s)} = \frac{k_p s + k_i}{s^2 + k_p s + k_i}, \tag{9}$$

where k_p and k_i are the proportional and integral gain of the PI regulator in the PLL, respectively.

The transfer function of the modified PLL-based filter structure in Fig. 2(d) can be derived as:

1. when input ω_{ref} is zero, the system is exactly the same as normal PLL structure

$$H_{mPLL,1}(s) = \frac{\omega_{out}(s)}{\omega_{in}(s)} = \frac{k_p s + k_i}{s^2 + k_p s + k_i} = H_{PLL}(s); \tag{10}$$

2. when input ω_{in} is zero

$$H_{mPLL,2}(s) = \frac{\omega_{out}(s)}{\omega_{ref}(s)} = \frac{s^2}{s^2 + k_p s + k_i}; \tag{11}$$

3. The final output can be calculated as

$$\omega_{out}(s) = H_{mPLL,1}(s) \cdot \omega_{in}(s) + H_{mPLL,2}(s) \cdot \omega_{ref}(s) \tag{12}$$

Similar to the improved LPF-based structure, introducing the reference speed ω_{ref} in the modified PLL may reduce the order of the input, which could be an advantage. Moreover, the modified PLL has similar filtering performance as the normal PLL when tracking a fixed speed reference. According to (12), the response of certain fixed speed reference $\omega_{ref}(t)$, i.e. the second term of the right part of (12), will converge to zero as time approaches infinity. Therefore, for fixed input reference, the transfer function of the modified PLL filter becomes the same as the normal PLL filter (9).

Fig. 4(a) illustrates the frequency response of $H_{PLL}(s)$, where f_c is 5 Hz with k_p=28 and k_i=100. The frequency response of a first order IIR LPF with the same cutoff frequency is illustrated as well. It can be seen that the PLL filter performs like a first order LPF when a fixed input reference speed is applied.

Since the PLL filter is a closed-loop filter, such structure should be able to provide enhanced accuracy. Regarding the PLL filter with normal structure (9), the error transfer function can be expressed as

$$E_{PLL}(s)=\frac{\varepsilon(s)}{\omega_{in}(s)}=\frac{s^2}{k_p s+k_i}. \quad (12)$$

And for ramp input $\omega_{in}=a_{in}\cdot t$, the error converges to

$$\lim_{t\to\infty}\varepsilon=\lim_{s\to 0}\left(s\frac{s^2}{k_p s+k_i}\cdot\frac{a_{in}}{s^2}\right)=0. \quad (13)$$

Thus, there is no ramp error for the PLL type filter.

For modified PLL structure, the error can be calculated as

$$\varepsilon(s)=\left(1-H_{PLL}(s)\right)\cdot\left(\omega_{in}(s)-\omega_{ref}(s)\right). \quad (14)$$

When the original speed to be filtered ω_{in} has an acceleration ratio close to that of the reference speed ω_{ref}, it can be obtained that

$$\omega_{in}(s)-\omega_{ref}(s)=\mathrm{L}\left\{\omega_{in}(t)-\omega_{ref}(t)\right\}=\mathrm{L}\left\{\Delta\omega\right\}=\frac{\Delta\omega}{s}. \quad (15)$$

Then, the error converges to

$$\lim_{t\to\infty}\varepsilon=\lim_{s\to 0}\left(s\frac{s^2}{s^2+k_p s+k_i}\cdot\frac{\Delta\omega}{s}\right)=0. \quad (16)$$

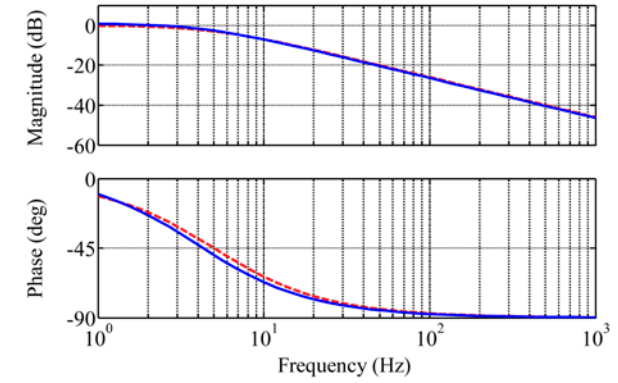

(a)

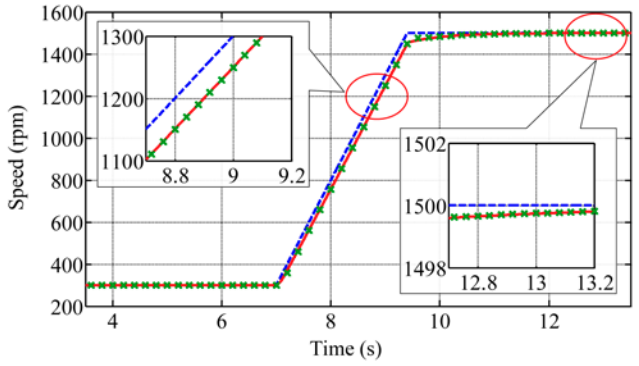

(b)

Fig. 4. PLL speed filters with k_p=28 and k_i=100 (f_c=5 Hz). (a) Frequency response comparison of different filters with f_c = 5 Hz, including PLL filter $H_{PLL}(s)$ (solid blue line) and first order LPF (red dashed line). (b) Simulated performance, including reference speed (blue dashed line), real speed (solid red line), and speed after PLL speed filter (green "x" marker).

It should be noticed that when ω_{ref} and ω_{in} have the same ramp slope, signal $\omega_{in}-\omega_{ref}$ is one order lower than ω_{in}.

The above analysis has shown that when a PLL is used for speed filtering, its characteristic is similar to a first order IIR LPF. The closed-loop structure with negative feedback and integral loop can compensate any possible error at steady-state as well as when tracking a ramp speed reference, achieving the same performance as the improved LPF-based structure. It should be noted that when k_i = 0 in the PLL, the transfer function (9) will degenerate to

$$H_{PLL}(s)=\frac{\omega_{out}(s)}{\omega_{in}(s)}=\frac{k_p}{s+k_p}, \quad (17)$$

which is a first order LPF whose cutoff frequency ω_c equals k_p. Therefore, the normal structure in Fig. 2(c) with k_i=0 can be implemented directly in the DSP system to form a digital first order LPF without analog-to-digital conversion and will not suffer from the coefficients quantization errors. However, when k_i=0, the normal PLL type filter degenerates to a first order LPF and the property of zero error for ramp input in (14) cannot be possessed anymore. While $k_i\neq 0$, there will be no ramp error, but extra phase delay may be introduced as shown in Fig. 4(a).

Fig. 4(b) shows the simulated performance of the normal structure PLL filter with 5 Hz cutoff frequency. It can be seen that there is no steady-state error at either steady-state conditions or during the ramp procedure. Therefore, using PLL filter can overcome the drawbacks of normal LPF.

An important feature of PLL type filter is that it has approximately linear relationship between its cutoff frequency f_c (bandwidth ω_c) and the values of the PI gains (k_p and k_i) of the PLL. This eases the on-line implementation of filters with adaptive cutoff frequency for improving the transient response.

Taking the normal PLL structure as an example, whose transfer function is expressed by (9), the cutoff frequency (bandwidth) is defined as the frequency where the magnitude is $1/\sqrt{2}$, i.e.

$$\left|H_{PLL}(j\omega_c)\right|=\left|\frac{k_p j\omega_c+k_i}{(j\omega_c)^2+k_p j\omega_c+k_i}\right|=\frac{1}{\sqrt{2}}. \quad (18)$$

By solving (19), it can be obtained that

$$\omega_c=\sqrt{\frac{k_p^2+2k_i+\sqrt{(k_p^2+2k_i)^2+4k_i^2}}{2}}. \quad (19)$$

To simplify the analysis, a linear relationship may be chosen to describe the relationship between k_p and k_i, e.g.

$$k_i=a\cdot k_p+b. \quad (20)$$

Substituting (21) into (20), and assuming $1/k_p$ is close to zero, ω_c in (20) can be approximated as

$$\omega_c\approx k_p+a. \quad (21)$$

A unit ratio between ω_c and k_p is obtained, which could also be an advantage when implementing the adaptive cutoff frequency control with fixed-point DSPs.

Fig. 5 shows the comparison of the bandwidth values obtained from (20) (the true values) and (22) (approximated using linear relationship) when k_p is changed from 10 to 300 while keeping k_i=5k_p (i.e. a=5 and b=0). The largest error of

0.07 Hz (3% with respect to the corresponding cutoff frequency of 2.32 Hz) is observed when k_p =10. This illustrates that the cutoff frequency estimation error caused by the approximation in (22) is very small and it is definitely acceptable to assume a linear relationship between ω_c and k_p for adaptive cutoff frequency control.

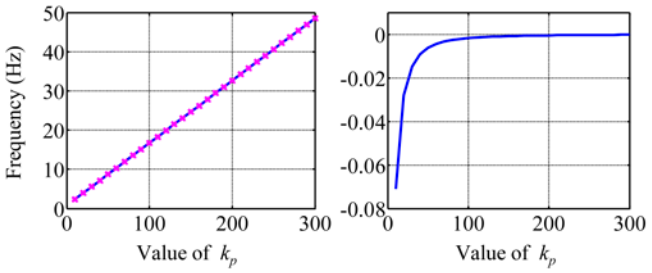

Fig. 5. PLL type filter characteristic with $k_i = 5k_p$. (a) Cutoff frequency f_c vs. k_p, including real bandwidth (blue solid line), and the linear approximation (magenta 'x' markers). (b) Cutoff frequency error between real bandwidth and its linear approximation.

A simple tuning strategy to implement the adaptive cutoff frequency control is to vary the values of the PI gains linearly according to the error between the reference speed (ω_{ref}) and the filtered estimated speed (ω_{out}), i.e.

$$k_p = c \cdot \left| \omega_{out}(t) - \omega_{ref}(t) \right| + d \ . \tag{22}$$

When there is a speed transient, e.g. caused by a step load on, the estimated speed (ω_{out}) will drop and differ from the reference speed (ω_{ref}). As the difference increases, k_p will increase and consequently the cutoff frequency of the speed filter, so that a fast response to the transient can be achieved. For an example of c=200 and d=100, 1.0 rad/s speed difference will triple the value of k_p (from 100 to 300), while the cutoff frequency is approximately tripled as well.

V. Experimental Verification

A flux linkage based position estimation algorithm, which is presented in details in [9] and the speed information is obtained from a position PLL, is implemented together with the proposed speed filters to verify their performances. Fig. 6 shows the experimental setup. The SynRM is driven by an inverter controlled by a DSP. A servo PMSM is used to apply load torque to the SynRM. The parameters of the SynRM are given in Table I. The switching frequency is set to 10 kHz and the signal sampling is performed at the beginning of each switching period.

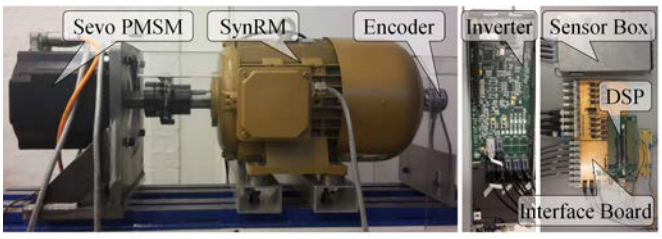

Fig. 6. Experimental setup.

TABLE I
Synchronous Reluctance Machine Parameters

Rated power	5.5 kW	Stator resistance	0.38 Ω
Rated current	13.9 A	d-axis inductance	124.0 mH
Rated speed	1500 rpm	q-axis inductance	36.2 mH
Rated torque	35.0 N·m	Pole pairs	2
Rated frequency	50 Hz	Inertia	1.9×10^{-2} kg·m^2

First, the real position and speed information from a mechanical encoder is used in the FOC. The estimated position and speed information at different operation conditions are shown in Fig. 7. The experimental results show that the position estimation is already good, while the estimated speed from the position PLL is still noisy due to the large PI gains used in the position PLL in order to handle fast mechanical dynamics, such as step load changes shown in Fig. 7(b). About 25 rpm peak-to-peak speed ripple can be observed in Fig. 7(a). It is worth to point out that the speed ripple contains significant sixth order harmonic component, which may mainly be caused by the imperfect inverter voltage drop compensation. If such estimated speed is used directly as the speed feedback for sensorless control, the speed estimation will become worse in steady-state with the peak-to-peak ripple increased to about 60 rpm and the system performance demonstrated in the experiment is not satisfactory. Thus, an extra speed filter is needed in order to improve the system performance.

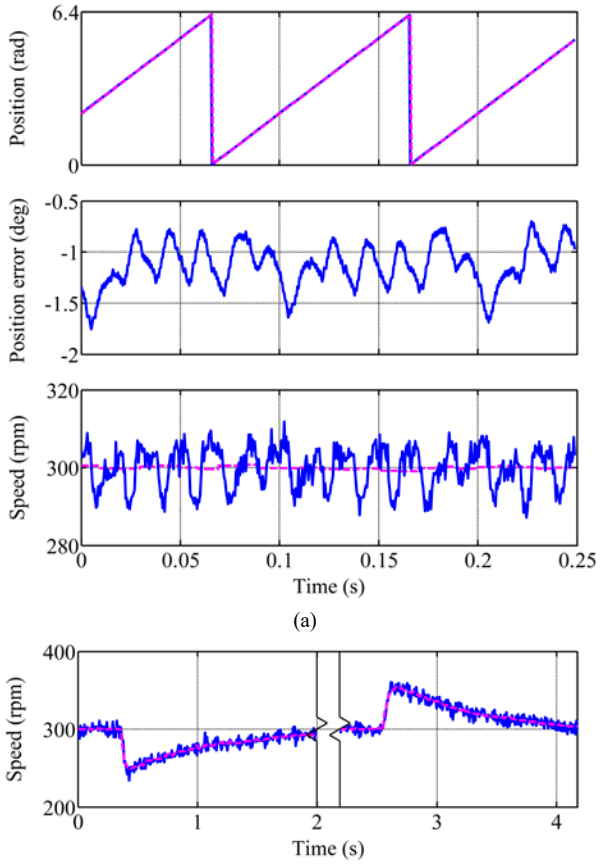

Fig. 7. Sensored FOC experimental results without speed filter, including real position/speed (magenta dashed line), and estimated position/speed (solid blue line). (a) 300 rpm no load. (b) Step load on and off at 300 rpm.

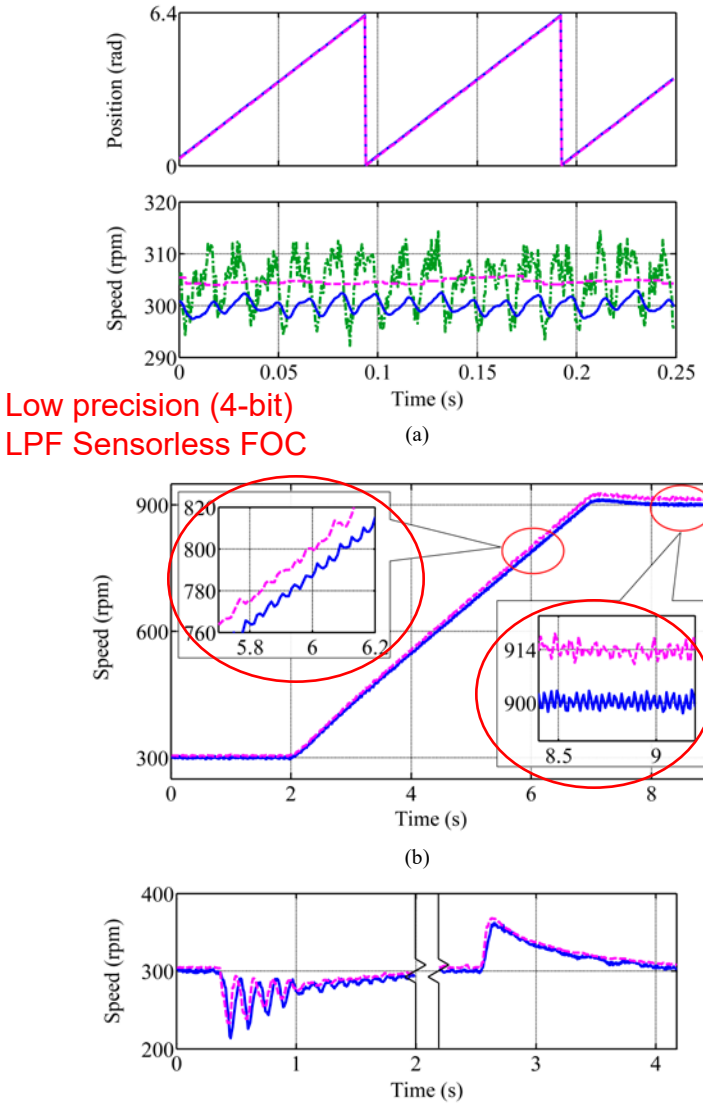

Fig. 8. Sensorless FOC test results with first order LPF, including real position/speed (magenta dashed line), original estimated speed (green dash-dot line), and estimated position or filtered estimated speed (solid blue line). (a) 300 rpm no load. (b) Speed ramp up. (c) Step load on and off at 300 rpm.

Fig. 8 shows the experimental results of full sensorless operation of the drive, when a first order LPF with low-precision filter coefficients (four significant figures which introduce about 0.01% error of the coefficient values) is used to filter the estimated speed. The cutoff frequency of the LPF is set to be 17.5 Hz, with the purpose of achieving better system response during the speed transients. It can be seen in Fig. 8(a) that the position estimation is still accurate, and the average values of the real and estimated speeds can match as well. But there is about 5 rpm error between the average values of the real speed and the filtered estimated speed. However, the filtered estimated speed is much smoother than the original estimated speed. Fig. 8(b) shows the speed information when ramping up to 900 rpm. It can be seen that speed error exists during both ramp and steady-state conditions, and there is about 14 rpm speed error at 900 rpm. Since the filtered estimated speed serves as the speed feedback, which will be forced by the controller to reach the reference speed of 900 rpm, the real speed is higher than 900 rpm as can be seen in Fig. 8(b). Besides, it can be seen in Fig. 8(c) that the speed transient performance becomes worse at full-sensorless operating condition. Speed oscillation during step load on transient was observed, which may be due to the increased dc-link voltage variation (when loaded) of the specific drive system under test [21].

Fig. 9 shows the test results with improved structure of the first order LPF, with same filter coefficients used for the test shown in Fig. 8. It can be seen that the speed errors visualized in Fig. 8(a) and (b) have now been removed as shown in Fig. 9. In the meantime, the dynamic performance during step load shown in Fig. 9(c) exhibits no significant different compared to the results given in Fig. 8(c).

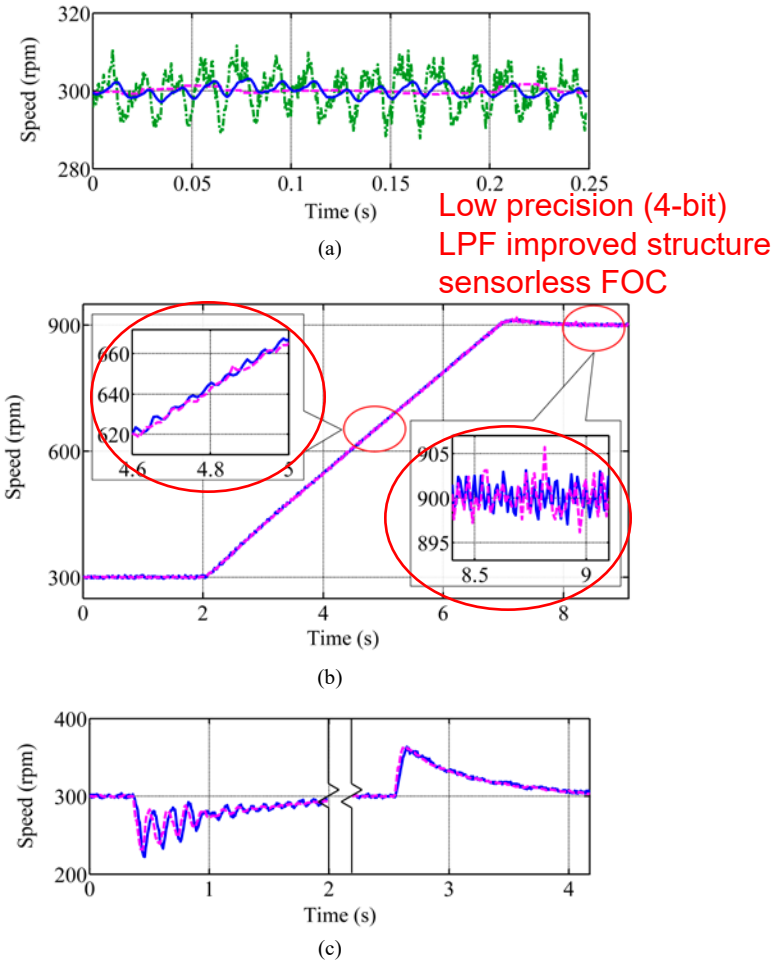

Fig. 9. Sensorless FOC test results with improved structure of first order LPF, including real speed (magenta dashed line), estimated speed (green dash-dot line), and estimated position or filtered estimated speed (solid blue line). (a) 300 rpm no load. (b) Speed ramp up. (c) Step load on and off at 300 rpm.

Fig. 10 shows the sensorless FOC experimental performance of the modified PLL filter at different operating conditions. The PI parameters of the LF are set to be $k_p = 100$ and $k_i = 1000$, which gives a cutoff frequency of 17.5 Hz. It can be seen from Fig. 10(a) and (b) that it demonstrates similar results to those achieved by the improved LPF-based structure in steady-state and when tracking a ramp speed reference.

It can be seen in Fig. 10(c) that the oscillation is higher than the first order LPF during step load on transient, which is reasonable as the phase delay of the PLL filter is higher than the first order LPF when k_i is greater than zero as shown in Fig. 4(a). However, it is much easier and costless for the PLL type speed filters to achieve adaptive cutoff frequency control as discussed previously. Fig. 10(d) shows the step load performance of the PLL speed filter with adaptive cutoff frequency by setting c=200 and d=100 in (23). The integral gain k_i is chosen to be k_i=2.5k_p+750. It can be seen from Fig. 10(d) that the dynamic performance improves a lot compared with Fig. 8(c), Fig. 9(c), and Fig. 10(c).

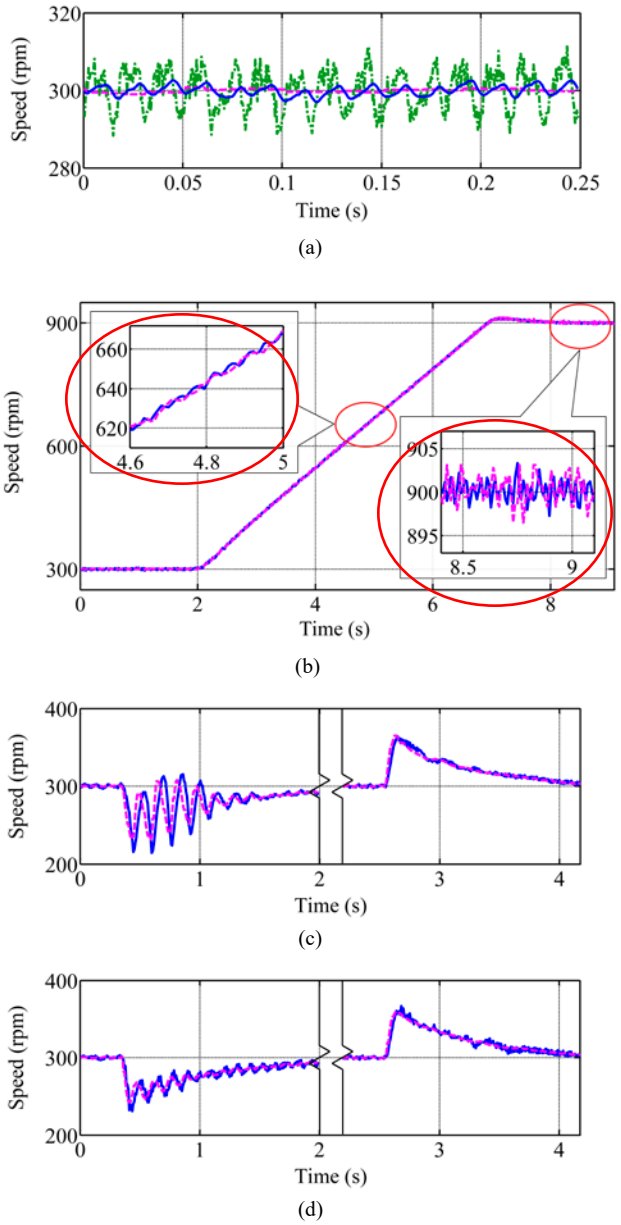

Fig. 10. Sensorless FOC test results with modified PLL speed filter, including real position/speed (magenta dashed line), estimated speed (green dash-dot line), and estimated position or filtered estimated speed (solid blue line). (a) 300 rpm no load. (b) Speed ramp up with fixed cutoff frequency. (c) Step load on and off at 300 rpm with fixed cutoff frequency. (d) Step load on and off at 300 rpm with adaptive cutoff frequency

Fixed cutoff frequency gives large occilations
Adaptive cutoff frequency gives best performance for PLL

VI. Conclusion

A comparative study of the LPF and PLL type filters to serve as machine speed filter is carried out in this paper. The drawbacks of using conventional LPFs in the digital system are analyzed, including ramp reference tracking error, steady-state quantization errors, and complexity of on-line cutoff frequency adjustment. The situation will become worse when fixed-point DSP is adopted, which is widely used in mass production of the controllers. To improve the performance, an improved LPF-based structure is proposed, where the ramping and steady-state errors can be removed by reducing the order of input. Moreover, the PLL structure, which is rarely used for pure filtering function in the existing studies, is found to be a very good candidate, especially for speed filtering. First, it does not have ramping and steady-state errors. Furthermore, the theoretical analysis of the PLL type filter demonstrates that there is an approximately linear relationship between the values of the PI gains and its bandwidth, which makes it very easy to achieve adaptive cutoff frequency control for improving the system transient performance at different operating conditions. A simple tuning strategy to achieve adaptive cutoff frequency control is proposed as well. All the proposed filter topologies are verified experimentally on a sensorless SynRM drive system, and satisfactory performance can be achieved. The adaptive cutoff frequency control of the PLL type filter is proved to be useful and improved performance at step load change conditions can be observed.

When can it?

References

[1] P. P. Acarnley and J.F. Watson, "Review of position-sensorless operation of brushless permanent-magnet machines," *IEEE Trans. Ind. Electron.*, vol. 53, no. 2, pp. 352–362, Apr. 2006.

[2] F. Briz and M. W. Degner, "Rotor position estimation: A review of high frequency methods," *IEEE Ind. Electron. Mag.*, vol. 5, no. 2, pp. 24–36, Jun. 2011.

[3] J. Holtz and J. T. Quan, "Drift and parameter compensated flux estimator for persistent zero stator frequency operation of sensorless controlled induction motors," *IEEE Trans. Ind. Appl.*, vol. 39, no. 4, pp.1052–1060, Jul./Aug. 2003.

[4] R. Wu and G. R. Slemon, "A permanent magnet motor drive without a shaft sensor," *IEEE Trans. Ind. Appl.*, vol. 27, no. 5, pp.1005–1011, Sep./Oct. 1991.

[5] P. L. Jansen and R. D. Lorenz, "Transducerless position and velocity estimation in induction and salient ac machines," *IEEE Trans. Ind. Appl.*, vol. 31, pp. 240–247, Mar./Apr. 1995.

[6] J. X. Shen, Z. Q. Zhu, and D. Howe, "Improved speed estimation in sensorless PM brushless AC drives," *IEEE Trans. Ind. Appl.*, vol. 38, no. 4, pp.1072–1080, Jul./Aug. 2002.

[7] L. Harnefors and H.-P. Nee, "A general algorithm for speed and position estimation of AC motors," *IEEE Trans. Ind. Electron.*, vol. 47, no. 1, pp. 77–83, Feb. 2000.

[8] O. Wallmark, L. Harnefors, and O. Carlson, "An improved speed and position estimator for salient permanent-magnet synchronous motors," *IEEE Trans. Ind. Electron.*, vol. 52, no. 1, pp. 255–262, Feb. 2005.

[9] T. F. Chan, W. Wang, P. Borsje, Y. K. Wong, and S. L. Ho, "Sensorless permanent-magnet synchronous motor drive using a reduced-order rotor flux observer," *IET Electr. Power Appl.*, vol. 2, No. 2, pp. 88–98, Mar. 2008.

[10] S. C. Agarlita, I. Boldea, and F. Blaabjerg, "High-frequency-injection -assisted "active flux"-based sensorless vector control of reluctance synchronous motors, with experiments from zero speed," *IEEE Trans. Ind. Appl.*, vol. 48, no. 6, pp. 1931–1939, Nov./Dec. 2012.

[11] O. Wallmark, J. Galic, and H. Mosskull, "Sensorless control of PMSMs adopting indirect self-control," *IET Electr. Power Appl.*, vol. 6, no. 1, pp. 12–18, 2012.

[12] T. Tuovinen and M. Hinkkanen, "Adaptive full-order observer with high-frequency signal injection for synchronous reluctance motor drives," *IEEE Journal on Emerging and Selected Topic in Power Electronics*, vol. 2, no. 2, pp.181–189, Jun. 2014.

[13] Y. D. Yoon, S. K. Sul, and K. Ide, "High-bandwidth sensorless algorithm for AC machine based on square-wave-type voltage injection," *IEEE Trans. Ind. Appl.*, vol. 47, no. 3, pp. 1361–1370, May/Jun. 2011.

[14] G. Xie, K. Lu, S. K. Dwivedi, J. R. Rosholm, and F. Blaabjerg, "Minimum-voltage vector injection method for sensorless control of PMSM for low-speed operations," *IEEE Trans. Power Electron.*, vol. 31, no. 2, pp. 1785–1794, Feb. 2016.

[15] M. Schroedl, "Sensorless control of AC machines at low speed and standstill based on the 'INFORM' method," in *Proc. Conf. Record 1996 IEEE 31st IAS Annual Meeting*, Oct. 1996, vol. 1, pp. 270–277.

[16] T.-S. Kwon, S.-K. Sul, H. Nakamura, and K. Tsuruta, "Identification of the mechanical parameters for servo drive," *Conf. Rec. IEEE 41st IAS Annu. Meeting*, vol. 2, pp. 905–910, Oct. 2006.

[17] C. M. Rader and B. Gold, "Digital Filter Design Techniques in the Frequency Domain," in *Proc. of IEEE*, vol. 55, pp. 149–171, Feb. 1967.

[18] S. W. Smith, "Digital Signal Processors," in *The Scientist and Engineer's Guide to Digital Signal Processing*, San Diego: California Technical Publishing, 1999, pp. 503–534.

[19] Z. Wang, K. Lu, and F. Blaabjerg, "A simple startup strategy based on current regulation for back-EMF-Based sensorless control of PMSM," *IEEE Trans. Power Electron.*, vol. 27, no. 8, pp. 3817–3825, Aug. 2012.

[20] R. Teodorescu, M. Liserre, and P. Rodriguez, "Grid synchronization in single-phase power converters," in *Grid Converters for Photovoltaic and Wind Power Systems*, New York: Wiley-IEEE Press, 2011, pp. 43–91.

[21] D. Wang, K. Lu, P. O. Rasmussen, L. Mathe, and Y. Feng, "Analysis of voltage modulation based active damping techniques for small dc-link drive system," in *Proc. ECCE*, Montreal, Canada, Sep. 2015, pp. 2927–2934.

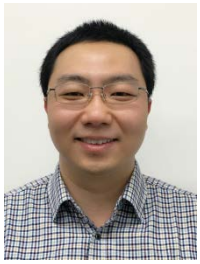

Dong Wang (S'13–M'16) was born in China in 1982. He received the B.S. degree in electrical engineering from Zhejiang University, Zhejiang, China, in 2004, and the M.S. and Ph.D. degrees from Aalborg University, Denmark, in 2006 and 2016, respectively.

From 2006 to 2012, he worked in industry, in Grundfos R&D China, Suzhou, China, as a Senior Motor Engineer. From 2016 to 2017, he was a Postdoc Researcher with the Department of Energy Technology, Aalborg University, Denmark. Since 2017, he has been an Assistant Professor with the same department. His research interests include design and control of synchronous reluctance and permanent magnet machines.

Kaiyuan Lu (M'11) received the B.S. and M.S. degrees from Zhejiang University, Zhejiang, China, in 1997 and 2000, respectively, and the Ph.D. degree from Aalborg University, Aalborg, Denmark, in 2005.

In 2005, he became an Assistance Professor in the Department of Energy Technology, Aalborg University, where since 2008, he has been an Associate Professor. His research interests include design of permanent magnet machines, FEM analysis, and control of permanent magnet machines.

Peter Omand Rasmussen (M'98) was born in Aarhus, Denmark, in 1971. He received the M.Sc.E.E. and Ph.D. degrees from Aalborg University, Aalborg, Denmark, in 1995 and 2001, respectively. In 1998, he became Assistant Professor, and in 2002, he became an Associate Professor at Aalborg University. His research areas are the design and control of switched reluctance, permanent-magnet machines and magnetic gears.

Zhenyu Yang (M'95) received the B.Sc. and M.Sc. degrees in control theory from Shandong University, China in 1991 and 1994, received the Ph. D. degree in control engineering from Beijing University of Aeronautics and Astronautics, China in 1998. He is currently associate professor at Department of Energy Technology at Aalborg University, Denmark.

His research interests include theory and application of fault detection and diagnosis, fault tolerant control, hybrid system modeling and control, nonlinear system identification and control, and industrial applications of advanced control theory and plant-wide automation for energy systems.